

See discussions, stats, and author profiles for this publication at: <https://www.researchgate.net/publication/302280806>

Mapping Forest Wildfire Risk of the World

Chapter · March 2015

DOI: 10.1007/978-3-662-45430-5_14

CITATIONS

19

READS

2,144

3 authors, including:



Ying Deng

Chinese Academy of Sciences

6 PUBLICATIONS 69 CITATIONS

[SEE PROFILE](#)



Peijun Shi

Beijing Normal University

301 PUBLICATIONS 8,226 CITATIONS

[SEE PROFILE](#)

Some of the authors of this publication are also working on these related projects:



climate change [View project](#)



Global Change Risk of Population and Economic Systems (GCR-PES): Mechanisms and Assessments [View project](#)

Mapping Forest Wildfire Risk of the World

Yongchang Meng, Ying Deng, and Peijun Shi

1 Background

Forest wildfire is one of the most severe natural hazards. It can start and spread quickly in an uncontrollable way and cause extensive losses and damages. Currently, the occurrence of forest wildfires around the world is over 200 thousand per year, with burned areas of 3.5–4.5 million km², which is approximately equal to the sum of the land areas of India and Pakistan and is greater than half of the land area of Australia (ISDR 2009). Forest wildfire is a hazard that causes the second-largest affected area over the world, following drought (ISDR 2009). Thus, forest wildfire poses a serious threat to national economic development, global ecological system, and personnel safety.

The simulation of forest wildfire propagation dynamically investigates the mechanism of fire spreading under different environmental conditions (topography, weather conditions, etc.) to forecast the fire spread direction and the final burned areas. Some models, such as the Rothermel model (Rothermel 1972) (USA) and the McArthur model (Noble et al. 1980) (Australia), are developed based on wildfire burning experiments and computer stimulations. These models exhibit good simulation results in specific areas but cannot

be applied globally. In addition, these models focus on the dynamic process in certain scenarios after a fire breaks out but unable to predict whether fires will occur in the future and assess its risk level.

The analysis of the causing factors of forest wildfire attempts to establish the correlation between fire features (probability of burning and burned area), natural factors (lightning, temperature, wind speed, topography, etc.), and socioeconomic factors (GDP, population, transportation, etc.), which can not only detect the drivers of forest wildfires in different regions but also can be used to assess the fire risk in different regions. Cruz et al. (2002) studied the relationship between natural factors (canopy height, wind speed, fuel moisture content etc.) and crown fire occurrences by using logistic regression analysis; Viegas et al. (2000) classified fuel types based on the measurements of plant moisture and discussed its relationship with the drought coefficient; Chuvieco et al. (2008) determined the relationship between the interannual variability of the unit area GDP and fire density on a global scale.

Satellite remote sensing and the monitoring of forest wildfires based on 3S techniques has been applied to identify active fire, predict fire propagation potential, and monitor burned area. Remote sensing has unique advantages in forest wildfire monitoring owing to its large spatial scale and temporal continuity of the images. Riano et al. (2007) used years of remote sensing data at 8-km-spatial resolution from the advanced very high resolution radiometer (AVHRR) to map the burned area at a global scale but unable to adequately monitor small-scale, lower-intensity fires due to the low saturation of the AVHRR images. Simon et al. (2004) compiled a global burned area map at a 1-km-spatial resolution by the interpretation of the along track scanning radiometer (ATSR-2) images. The ATSR images, however, underestimated the actual fire intensity, as they contain many forms of noise, such as high land temperature, gas combustions, and city lights. Moderate resolution imaging

Mapping Editors: Jing'ai Wang (Key Laboratory of Regional Geography, Beijing Normal University, Beijing 100875, China) and Fang Lian (School of Geography, Beijing Normal University, Beijing 100875, China).

Language Editor: Kai Liu (Key Laboratory of Environmental Change and Natural Disaster, Ministry of Education, Beijing Normal University, Beijing 100875, China).

Y. Meng · Y. Deng
Academy of Disaster Reduction and Emergency Management,
Ministry of Civil Affairs and Ministry of Education,
Beijing Normal University, Beijing 100875, China

P. Shi (✉)
State Key Laboratory of Earth Surface Processes and Resource
Ecology, Beijing Normal University, Beijing 100875, China
e-mail: spj@bnu.edu.cn

spectroradiometer (MODIS) fire products mark a milestone in the development of fire remote sensing monitoring, with their high spectral resolution, spatial resolution, and middle- and long-wave infrared bands designed specifically for the observation of actively burning fires, which greatly enhance the reliability of the MODIS fire products (Kaufman et al. 1998). Giglio et al. (2006) revealed the spatial pattern of global fire density by compiling MODIS fire products. Based on MODIS, the spatial resolution of the visible infrared imaging radiometer suit (VIIRS) images has increased to 750 m even 375 m, which is more favorable for fire monitoring and identification; however, the time series of the images is too short for further analysis since it was launched in 2011.

Previous studies mainly focus on the identification of active fire, the extraction of the burned area and the spatial-temporal patterns of fire density (van der Werf et al. 2006, 2010; Giglio et al. 2013), lacking of in-depth research studies on forest wildfire risk assessment of different regions in the future. Thus, this study performs a quantitative assessment and mapping of forest wildfire risk at the global scale by compiling relatively long time series data acquired from MODIS products.

2 Method

Figure 1 shows the technical flowchart for mapping forest wildfire risk of the world.

2.1 Disaster System Theory of Forest Wildfire

According to natural disaster system theory, disasters are integrations of environments, exposures, and hazards (Shi 1991, 1996, 2002). The hazard of forest wildfire disaster is fire, including both man-made and natural fires. The hazard intensity can be measured by the fire occurrence, fire intensity, burned area, flame height, and so on. This study selects annual frequencies of fire occurrence as the hazard intensity indicator. Exposures are the potential objects affected by forest wildfire hazards, such as vegetation, population, infrastructure, and agriculture. The susceptibility of exposures to forest wildfire is related to vulnerability, that is, more vulnerable corresponds to more probable to be damaged. The averaged burned area in a single fire is chosen as the vulnerability index. The hazard-formative environment denotes the particular topography and weather conditions that nurture and affect the occurrences and propagation of forest wildfire disasters. Therefore, a comprehensive understanding and investigation of the interactions of all three components are required to get a better understanding of global forest wildfire risk distribution.

2.2 Forest Wildfire Risk

The forest wildfire risk is assessed with a $0.1^\circ \times 0.1^\circ$ grid cell which contains the land cover types of forest (Appendix III, Exposures data 3.19). In this study, six types of land

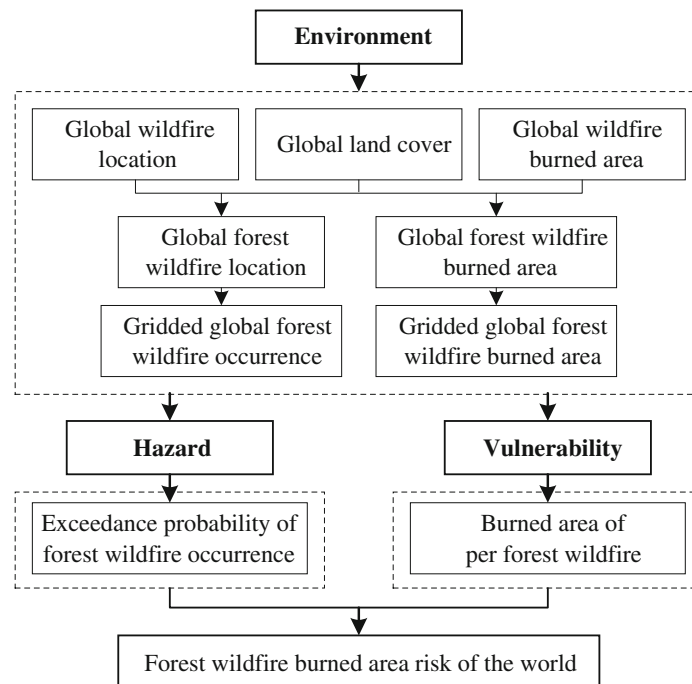


Fig. 1 Technical flowchart for mapping forest wildfire risk of the world

cover were selected as forest: evergreen needle leaf forest, evergreen broadleaf forest, deciduous needle leaf forest, deciduous broadleaf forest, mixed forests, and closed shrub lands.

2.2.1 Intensity

This study assumes that the forest wildfire is a stochastic Markov Process, and its state changes according to a transition rule that only depends on the known past N years' state.

As aforementioned, this study uses the annual forest wildfire occurrence as the indicator of hazard intensity and uses the historical forest wildfire occurrence to conduct the assessment. The time series of grid global forest wildfire occurrence dataset acquired from MODIS (Appendix III, Hazards data 4.16) is too short ($N = 12$) to analyze using the traditional extreme value fitting theories. The information diffusion theory is therefore introduced to cope with this problem. Information diffusion theory is a fuzzy mathematic method that makes the dataset elements set valued by taking advantage of the fuzzy information optimally (Huang 1997). This study applies normal information diffusion model—one of the most widely used models for calculating the return periods of hazards with different intensities developed by Huang (2012)—to the assessment of forest wildfire hazard.

2.2.2 Vulnerability

We calculated the fire occurrence and the corresponding burned area (Appendix III, Disasters data 5.8) of each cell to obtain the average burned area per fire as the vulnerability indicator. Here, the vulnerability reflects the sensitivity of the forest in different regions to fires: high vulnerability indicates that one or a few fires can easily cause large-scale forest wildfires, while in areas of low vulnerability, even a high fire occurrence may not lead to large-scale forest wildfires.

2.2.3 Risk

The assessment of hazard and vulnerability is based on the historical recorded data which has already taken the amplification or reduction effect of environments into account. Therefore, in the further assessment of forest wildfire risk, we can use Eq. (1) to obtain the approximate forest wildfire risk as follows:

$$R = H \times V \times E \approx H' \times V' \quad (1)$$

where H denotes the hazard, V denotes the vulnerability, E denotes the environments, and H' and V' denote the hazard and the vulnerability impacted by environments, respectively.

3 Results

3.1 Hazard Intensity

The global forest wildfire occurrence distribution of different return periods is generated in this study. The high-occurrence regions are mainly distributed in central South America, southwest of the Gulf of Mexico, northwest of Southeast Asia, and the central and western regions of Africa. The fire occurrence in these areas is almost over 100 times per year, even more than 1,000 times per year for some regions such as central South America, southern edge of rainforest located in Brazil and Bolivia, as well as Sierra Leone in West Africa. High fire occurrence in forest areas is scattered in the eastern and western coastal areas of Mexico, the northwestern area of the USA, the central part of Canada, the Russian Far East and eastern China, and southeastern Australia. Low forest wildfire occurrence areas are mainly found in northwestern Europe, northern Siberia, southwest China, northern and eastern areas of Canada, and inaccessible regions near the equatorial rainforest areas.

3.2 Vulnerability

The world forest areas with a relatively high vulnerability to forest wildfire are mainly concentrated in the regions of central Africa, southwestern Europe, southcentral and eastern areas of Siberia, midwest Canada, and central South America. In specific, the vulnerability of midwest Canada, northern Bolivia, and northeast China into Russia as well as the border of the Democratic Republic of Congo with Angola is particularly high, with a burned area per fire of 25 km² (2,500 ha) or more.

3.3 Risk

World forest wildfire risk maps were generated under different return periods. The high risk of forest wildfires mainly concentrated in central Africa, central South America, northwestern Southeast Asia, mid-eastern Siberia, and the northern regions of North America. The junction regions of the three African countries of the Democratic Republic of Congo, Republic of Angola, and the Republic of Zambia, along with Myanmar, Thailand, Laos, Cambodia, Bangladesh, Russia Far East, and the eastern coastal areas of Australia, North America, Mexico, Canada, Brazil, Bolivia, and Argentina, are high-risk areas for forest wildfires. The forest wildfire risk of Sierra Leone in West Africa is low although it has a high forest wildfire occurrence, since it is

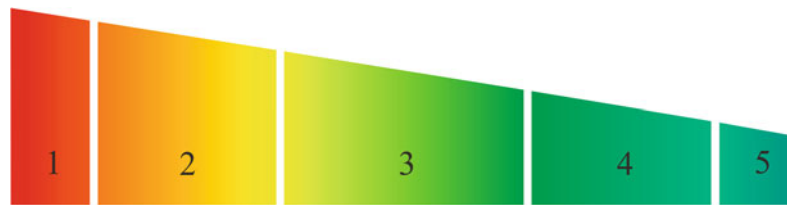


Fig. 2 Expected annual burned forest area risk of wildfire of the world. 1 (0, 10 %] Russia, Canada, Angola, Brazil, Congo (Democratic Republic of the), USA, Argentina, Burma, Bolivia, China, and Australia. 2 (10, 35 %] Mexico, South Sudan, Chad, India, Mongolia, Thailand, Laos, Vietnam, Zambia, Nigeria, Portugal, Cambodia, Indonesia, Spain, Paraguay, Guatemala, South Africa, Congo, Ethiopia, Cameroon, Nepal, Mali, North Korea, Central African Republic, Uganda, Sudan, and Venezuela. 3 (35, 65 %] Benin, Greece, Kazakhstan, Chile, Papua New Guinea, Romania, Madagascar, Japan, Honduras, Bangladesh, Mozambique, Colombia, France, Belarus,

Cuba, Tanzania, Guinea, Ukraine, Gambia, Peru, Zimbabwe, Senegal, Sierra Leone, Malawi, Belize, Philippines, The Republic of Côte d'Ivoire, Albania, Italy, Nicaragua, Bhutan, and Rwanda. 4 (65, 90 %] Costa Rica, Burkina Faso, Botswana, Lesotho, Syria, Liberia, Sweden, Norway, Dominican Republic, Guyana, UK, Croatia, Bosnia and Herzegovina, Swaziland, Sri Lanka, Algeria, Kenya, Uruguay, Bahamas, Slovenia, Serbia, Timor-Leste, Latvia, Malaysia, Ireland, and Montenegro. 5 (90, 100 %] Suriname, Guinea-Bissau, Iran, South Korea, Ghana, Pakistan, Hungary, Estonia, and Comoros, Macedonia

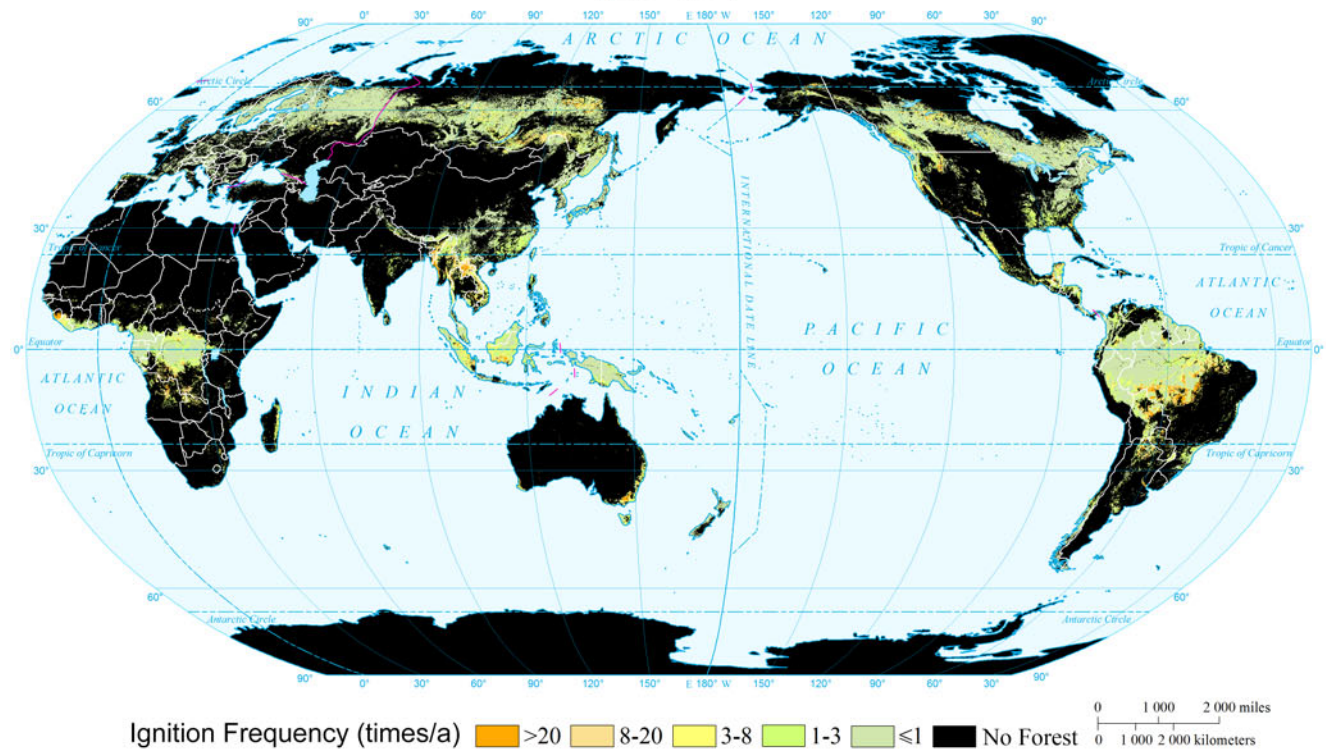
located in a tropical rainforest climate region with numerous thunderstorms, which contributes to the high forest wildfire occurrence, but simultaneously, the abundant rainfall helps to keep the forest wildfire spread under control.

By zonal statistics of the expected risk result, the expected annual burned forest area risk of wildfire of the world at national level is derived and ranked (Fig. 2). The top 1 % country with the highest expected annual burned

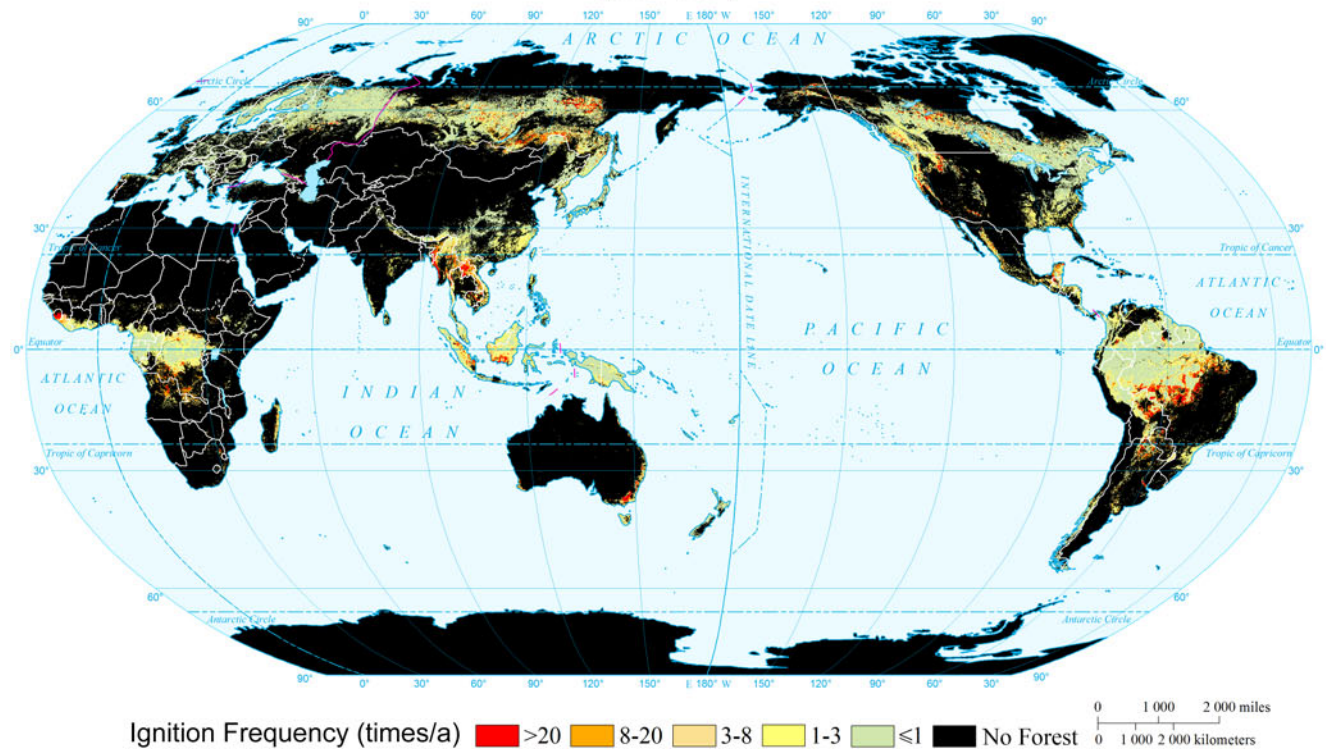
forest area risk of wildfire is Russia, and the top 10 % countries are Russia, Canada, Angola, Brazil, the Democratic Republic of Congo, the USA, Argentina, Burma, Bolivia, China, and Australia.

4 Maps

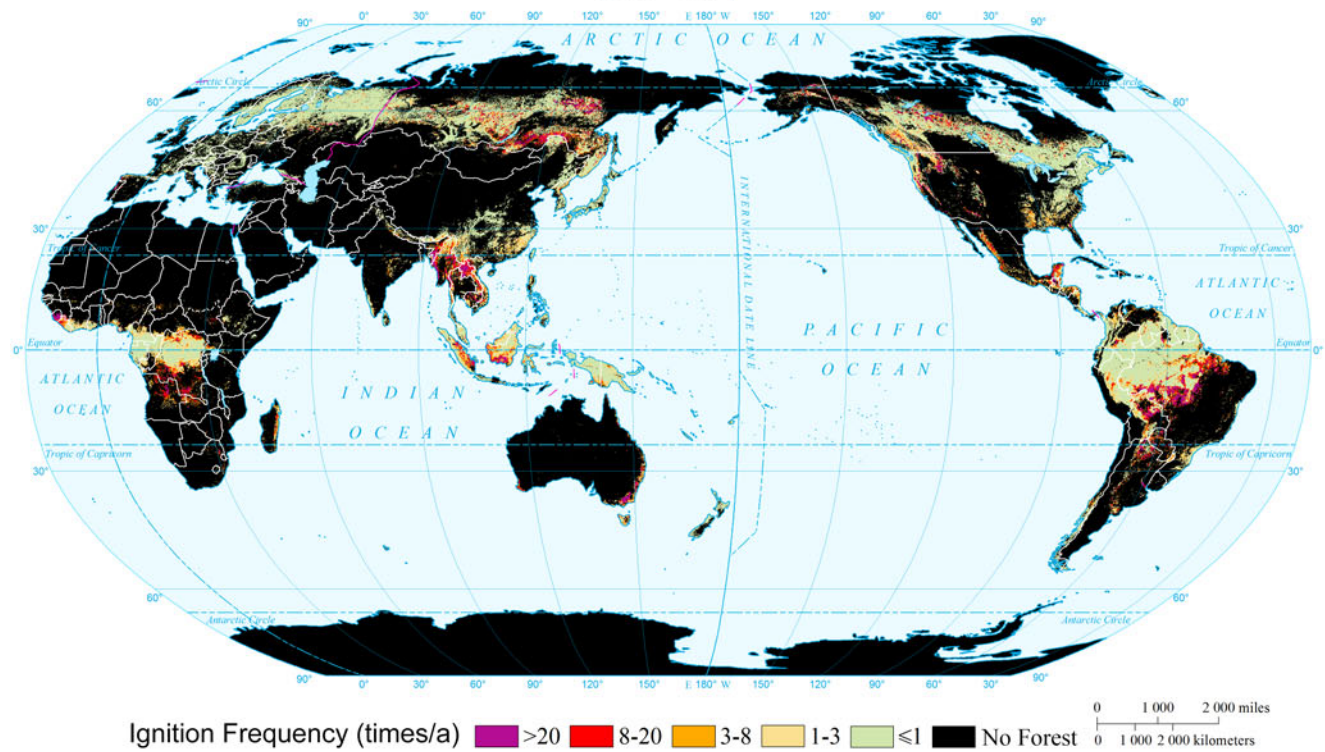
Global Intensity of Forest Wildfire by Return Period (10a)
($0.1^{\circ} \times 0.1^{\circ}$)



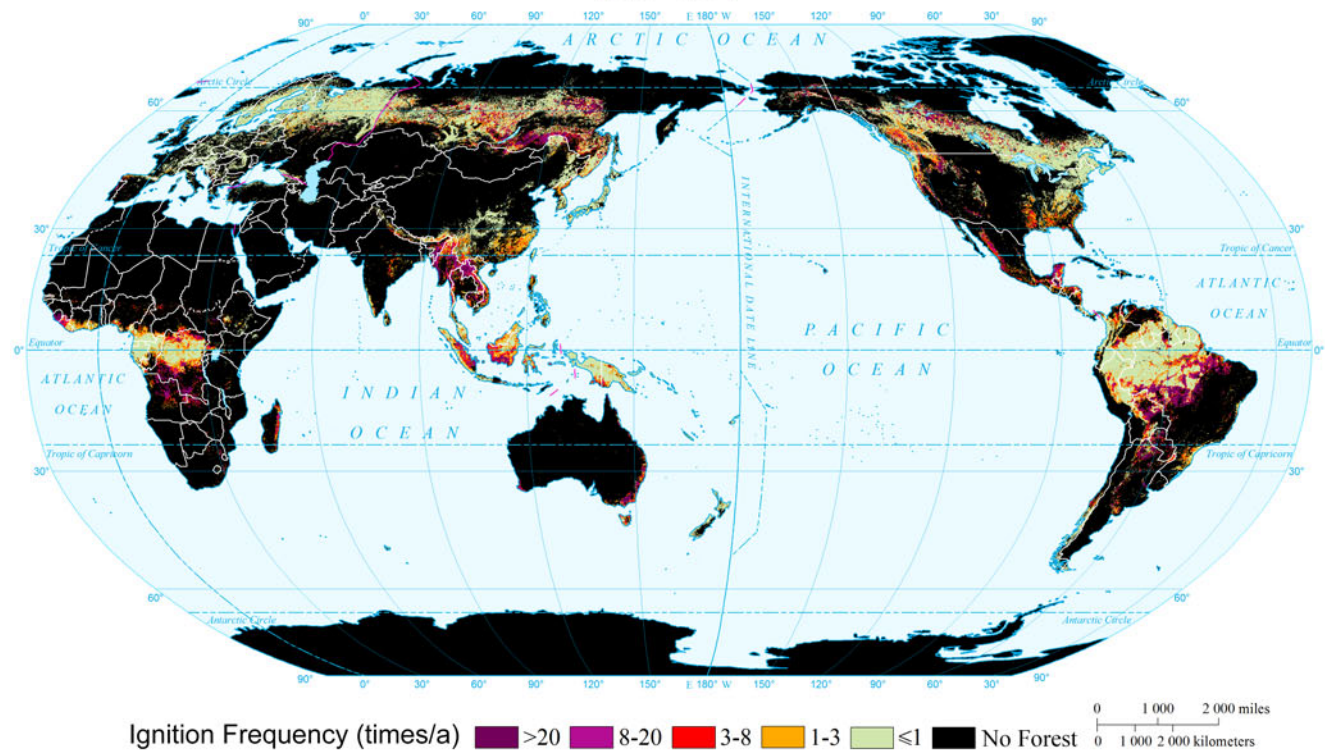
Global Intensity of Forest Wildfire by Return Period (20a)
($0.1^{\circ} \times 0.1^{\circ}$)



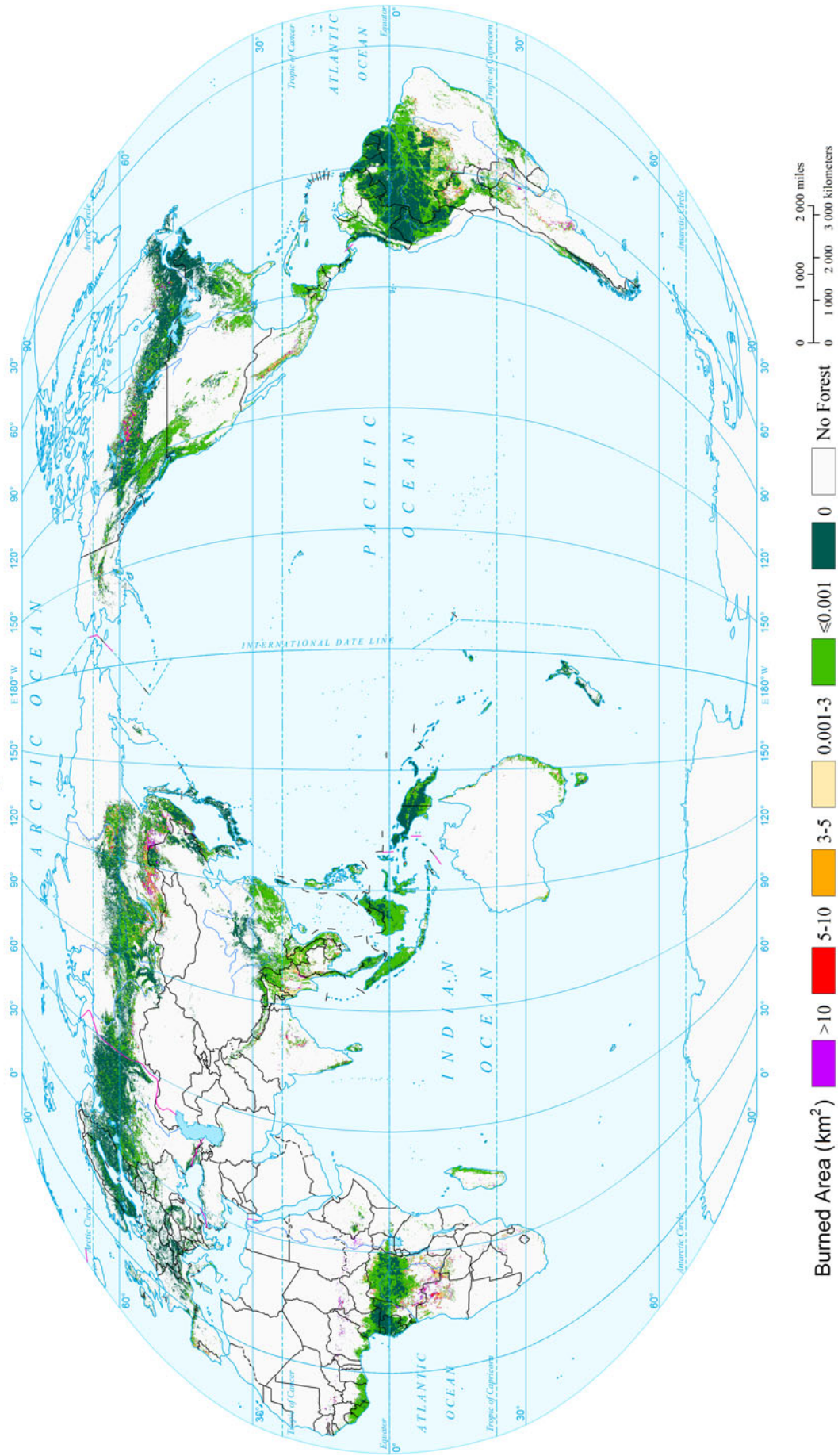
Global Intensity of Forest Wildfire by Return Period (50a)
($0.1^{\circ} \times 0.1^{\circ}$)



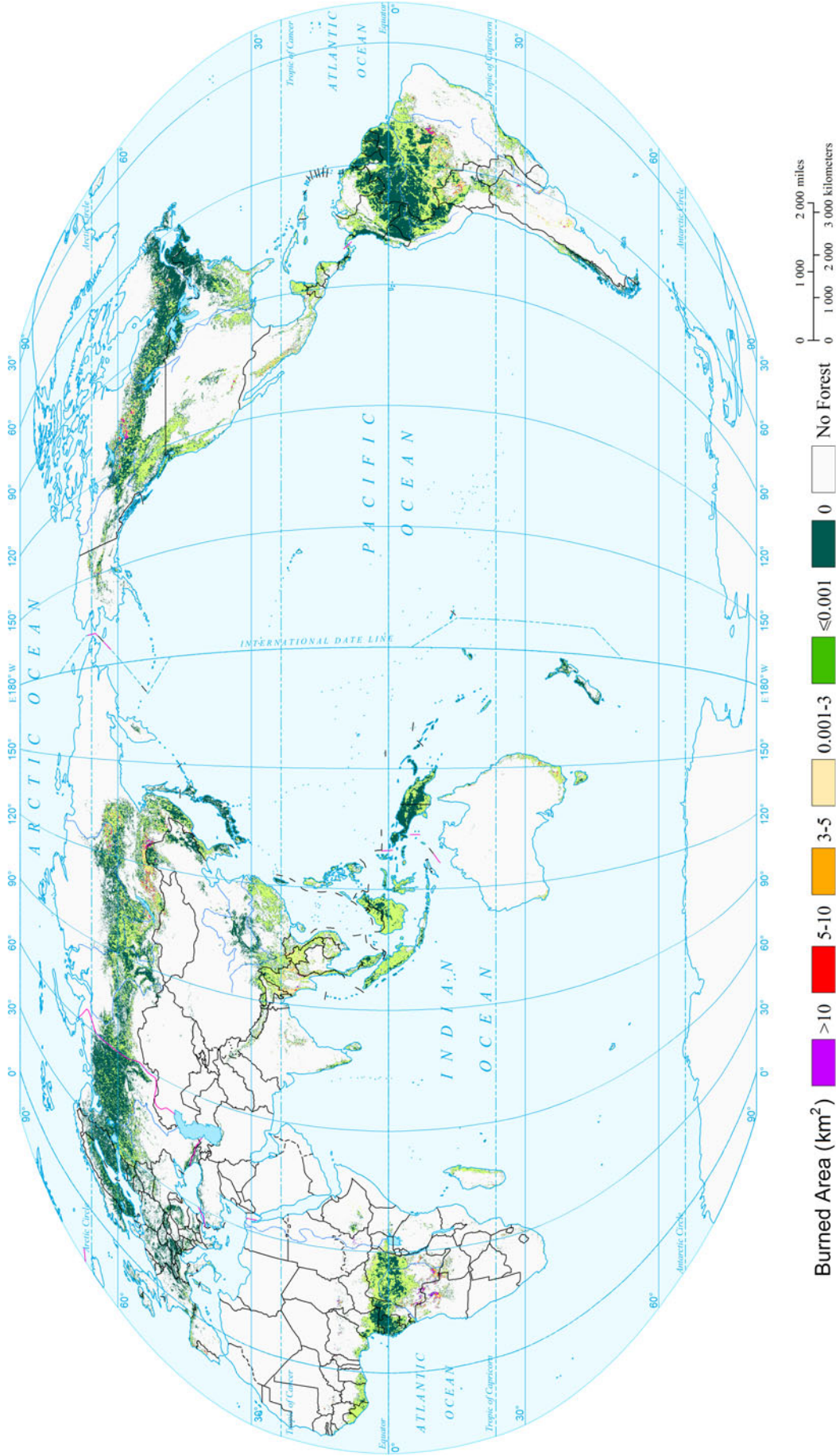
Global Intensity of Forest Wildfire by Return Period (100a)
($0.1^{\circ} \times 0.1^{\circ}$)



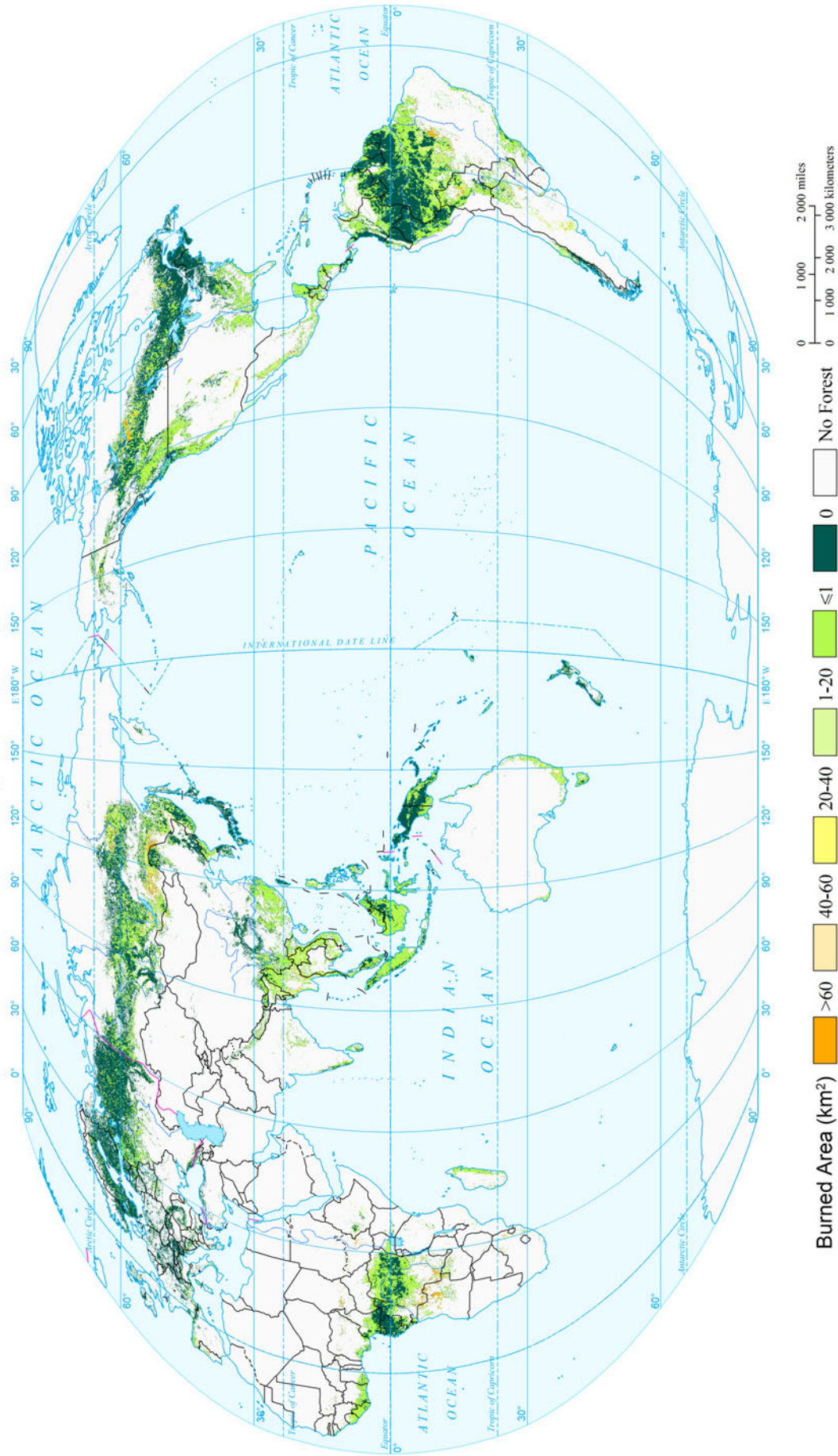
Average Annual Burned Area of Global Forest Wildfire (2001-2012)
(0.1°x0.1°)



Expected Annual Burned Area Risk of Forest Wildfire of the World
(0.1°x0.1°)



Burned Area Risk of Forest Wildfire of the World by Return Period (10a)
(0.1°×0.1°)



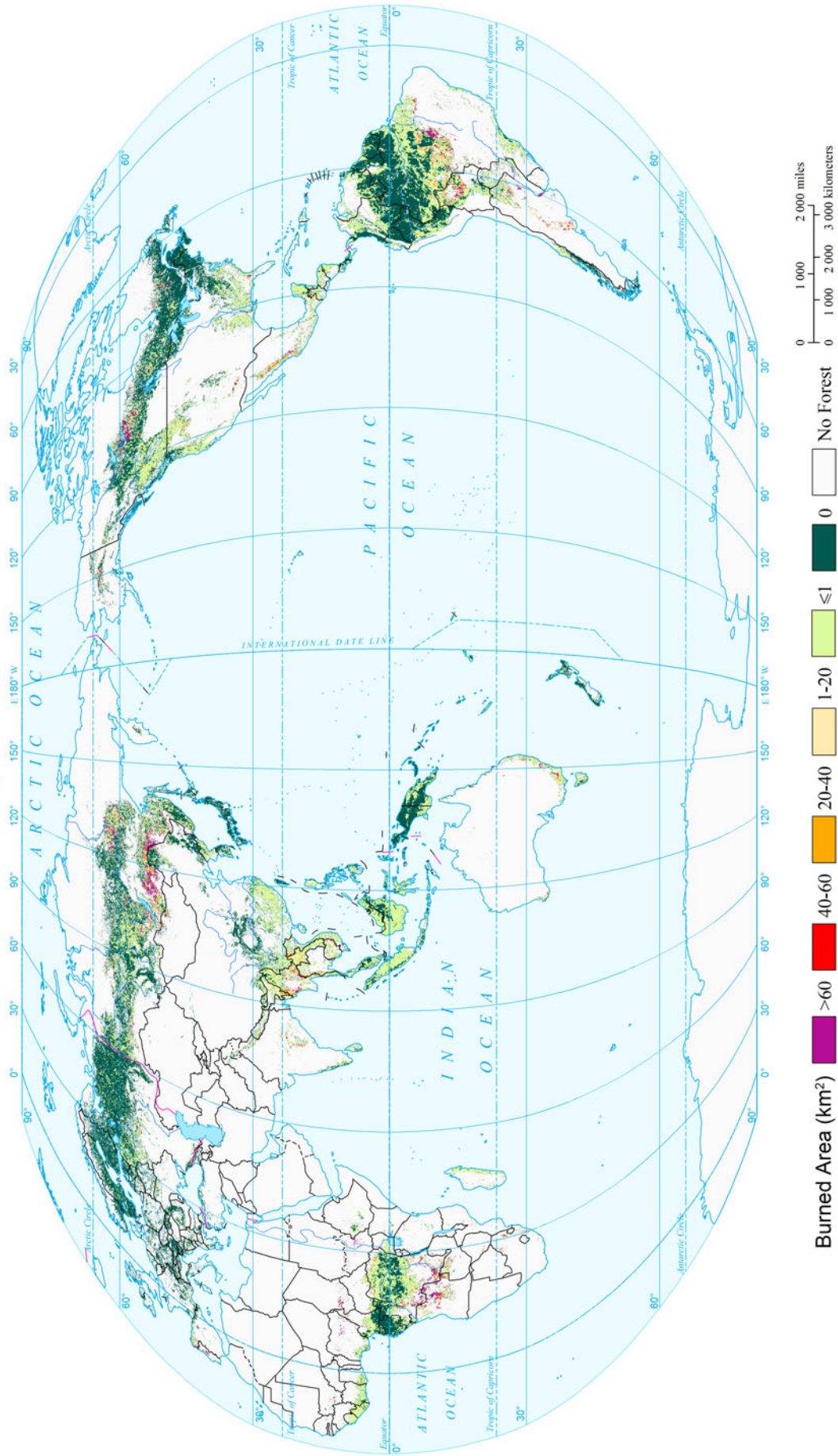
The map displays the global distribution of burned area between 1998 and 2003. The color scale indicates the intensity of burning, with red representing the highest values (>60 km²) and white representing no forest. Significant hotspots are visible in the Amazon basin, the Congo basin, and parts of Southeast Asia and Australia. The map also shows major oceans, latitude and longitude lines, and a legend for burned area and a scale bar.

Burned Area (km²)

- >60
- 40-60
- 20-40
- 1-20
- ≤1
- 0
- No Forest

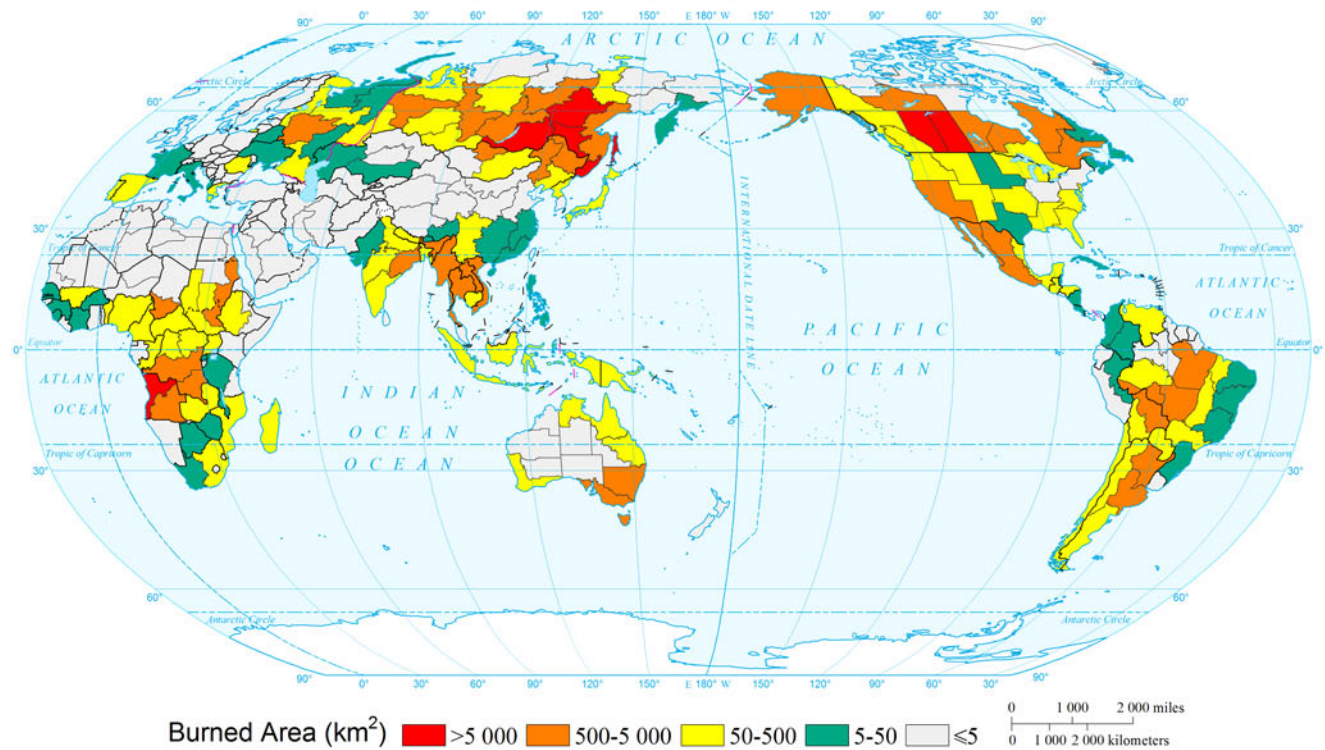
Scale: 0 to 2,000 miles / 0 to 3,000 kilometers

Burned Area Risk of Forest Wildfire of the World by Return Period (50a)
(0.1°×0.1°)

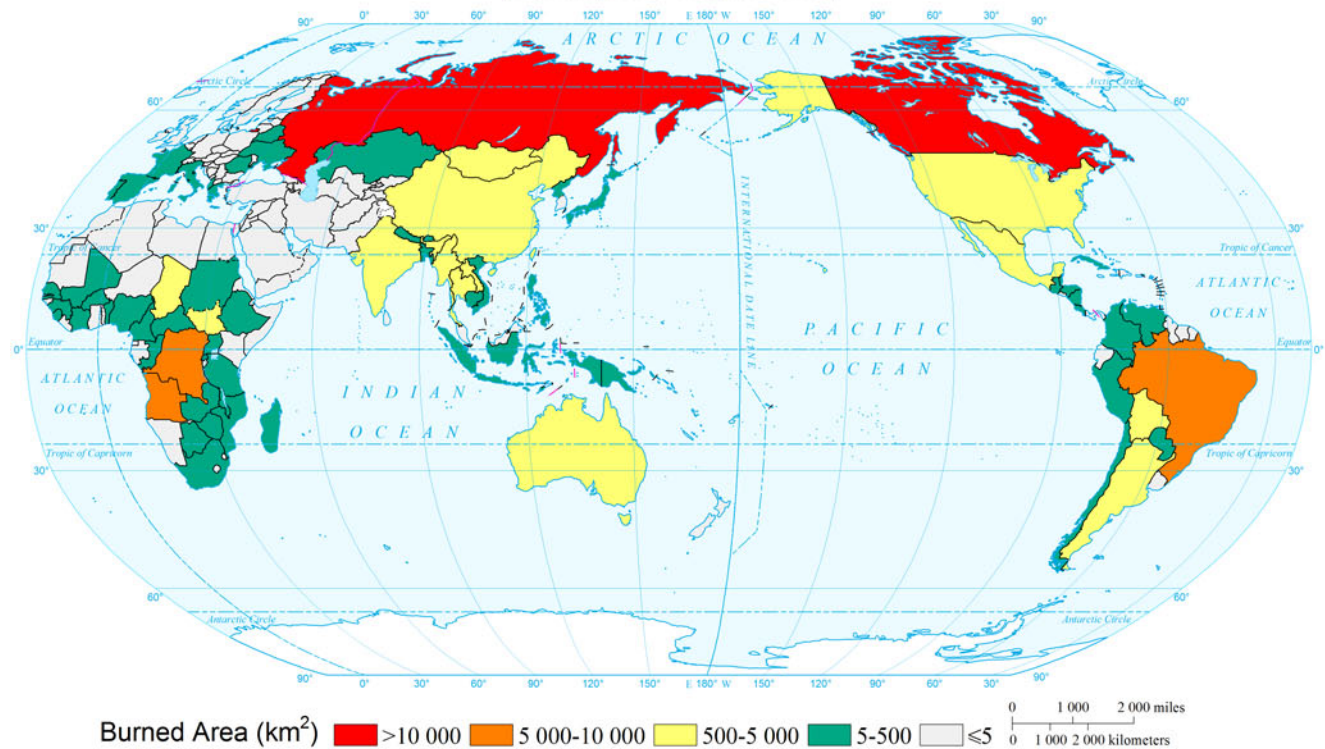


The map displays the global distribution of burned area between 1998 and 2003. The color scale indicates the area in square kilometers, with white representing 0 km², light yellow for 1-20 km², orange for 20-40 km², red for 40-60 km², and dark red for areas greater than 60 km². Significant concentrations of high burned area are visible in the Amazon basin of South America, the Congo basin in Central Africa, and various regions in Southeast Asia and Australia. The map also shows the Pacific, Atlantic, and Indian Oceans, as well as major latitude and longitude lines. A legend at the bottom right provides the color key and a scale bar in both miles and kilometers.

Expected Annual Burned Area Risk of Forest Wildfire of the World
(Comparable-geographic Unit)



Expected Annual Burned Area Risk of Forest Wildfire of the World
(Country and Region Unit)



References

- Chuvieco, E., L. Giglioand, and C. Justice. 2008. Global characterization of fire activity: Toward defining fire regimes from earth observation data. *Global Change Biology* 14: 1488–1502.
- Cruz, M.G., M.E. Alexander and R.H. Wakimoto. 2002. Predicting crown fire behavior to support forest fire management decision-making. In *Forest fire research and wildland fire safety*, ed. D.X. Viegas, 1–11. Rotterdam: Millpress.
- Giglio, L., I. Csizsarand and C.O. Justice. 2006. Global distribution and seasonality of active fires as observed with the terra and aqua moderate resolution imaging spectroradiometer (MODIS) sensors. *Journal of Geophysical Research: Biogeosciences* (2005–2012), 111(G2). doi:[10.1029/2005JG000142](https://doi.org/10.1029/2005JG000142).
- Giglio, L., J.T. Randersonand, and G.R. Werf. 2013. Analysis of daily, monthly, and annual burned area using the fourth-generation global fire emissions database (GFED4). *Journal of Geophysical Research: Biogeosciences* 118: 317–328.
- Huang, C.F. 1997. Principle of information diffusion. *Fuzzy Sets and Systems* 91: 69–90.
- Huang, C.F. 2012. *Natural disaster risk analysis and management*. Beijing: Science Press. (in Chinese).
- International Strategy for Disaster Reduction (ISDR). 2009. *Global assessment report on disaster risk reduction*. Geneva, Switzerland: United Nations.
- Kaufman, Y.J., C.O. Justiceand, L.P. Flynn, et al. 1998. Potential global fire monitoring from EOS-MODIS. *Journal of Geophysical Research: Atmospheres* (1984–2012) 103: 32215–32238.
- Noble, I.R., A.M. Gilland, and G.A.V. Bary. 1980. McArthur's fire-danger meters expressed as equations. *Australian Journal of Ecology* 5: 201–203.
- Riano, D., J.A. Moreno Ruizand, D. Isidoro, et al. 2007. Global spatial patterns and temporal trends of burned area between 1981 and 2000 using NOAA-NASA Pathfinder. *Global Change Biology* 13: 40–50.
- Rothermel, R.C. 1972. A mathematical model for predicting fire spread in wildland fuels: USDA Forest Service.
- Shi, P.J. 1991. Study on the theory of disaster research and its practice. *Journal of Nanjing University (Natural Sciences)* 11(Supplement): 37–42. (in Chinese).
- Shi, P.J. 1996. Theory and practice of disaster study. *Journal of Natural Disasters* 5(4): 6–17. (in Chinese).
- Shi, P.J. 2002. Theory on disaster science and disaster dynamics. *Journal of Natural Disasters* 11(3): 1–9. (in Chinese).
- Simon, M., S. Plummerand, F. Fierens, et al. 2004. Burnt area detection at global scale using ATSR-2: The GLOBSCAR products and their qualification. *Journal of Geophysical Research: Atmospheres* (1984–2012) 109(D14). doi:[10.1029/2003JD003622](https://doi.org/10.1029/2003JD003622).
- van der Werf, G.R., J.T. Randersonand, L. Giglio, et al. 2006. Interannual variability in global biomass burning emissions from 1997 to 2004. *Atmospheric Chemistry and Physics* 6: 3423–3441.
- van der Werf, G.R., J.T. Randersonand, L. Giglio, et al. 2010. Global fire emissions and the contribution of deforestation, savanna, forest, agricultural, and peat fires (1997–2009). *Atmospheric Chemistry and Physics* 10: 11707–11735.
- Viegas, D.X., G. Bovioand, A. Ferreira, et al. 2000. Comparative study of various methods of fire danger evaluation in southern Europe. *International Journal of Wildland Fire* 9: 235–246.